J|A|C|S
ARTICLES
Published on Web 08/26/2006

Kinetics of CO Insertion and Acetyl Group Transfer Steps, and a Model of the Acetyl-CoA Synthase Catalytic Mechanism

Xiangshi Tan, Ivan V. Surovtsev, and Paul A. Lindahl*

Contribution from the Departments of Chemistry and of Biochemistry and Biophysics, Texas A&M University, College Station, Texas 77843

Received May 10, 2006; E-mail: lindahl@mail.chem.tamu.edu

Abstract: Acetyl-CoA synthase/carbon monoxide dehydrogenase is a Ni−Fe−S-containing enzyme that catalyzes the synthesis of acetyl-CoA from CO, CoA, and a methyl group. The methyl group is transferred onto the enzyme from a corrinoid−iron−sulfur protein (CoFeSP). The kinetics of two steps within the catalytic mechanism were studied using the stopped-flow method, including the insertion of CO into a putative $Ni^{2+}-CH_3$ bond and the transfer of the resulting acetyl group to CoA. Neither step had been studied previously. Reactions were monitored indirectly, starting with the methylated intermediate form of the enzyme. Resulting traces were analyzed by constructing a simple kinetic model describing the catalytic mechanism under reducing conditions. Besides methyl group transfer, CO insertion, and acetyl group transfer, fitting to experimental traces required the inclusion of an inhibitory step in which CO reversibly bound to the form of the enzyme obtained immediately after product release. Global simulation of the reported datasets afforded a consistent set of kinetic parameters. The equilibrium constant for the overall synthesis of acetyl-CoA was estimated and compared to the product of the individual equilibrium constants. Simulations obtained with the model duplicated the essential behavior of the enzyme, in terms of the variation of activity with [CO], and the time-dependent decay of the NiFeC EPR signal upon reaction with CoFeSP. Under standard assay conditions, the model suggests that the vast majority of active enzyme molecules in a population should be in the methylated form, suggesting that the subsequent catalytic step, namely CO insertion, is rate limiting. This conclusion is further supported by a sensitivity analysis showing that the rate is most sensitively affected by a change in the rate coefficient associated with the CO insertion step.

Introduction

Acetyl-CoA synthases/carbon monoxide dehydrogenases are found in homoacetogenic bacteria, methanogenic archaea, and CO-utilizing hydrogenogenic bacteria.[1−4] These O_2-sensitive bifunctional enzymes allow such organisms to grow chemoautotrophically on simple inorganic compounds. The enzyme from the homoacetogen *Moorella thermoacetica* (ACS/CODH) has been studied most extensively.[5,6] The β subunits of this 310 kDa $\alpha_2\beta_2$ tetramer catalyze the reversible reduction of CO_2 to CO, while the α subunits catalyze the synthesis of acetyl-CoA from CO, CoA, and a methyl group donated from a corrinoid−iron−sulfur protein (CoFeSP). At a buffered pH, this is represented by reaction 1.

$$CO + CoA + CH_3-Co^{3+}FeSP \rightleftarrows CH_3-C(O)-CoA + Co^{1+}FeSP \quad K_{ACS} \quad (1)$$

The active site for this reaction, called the A cluster, consists of an $[Fe_4S_4]$ cubane bridged via a cysteine residue to a Ni ion called proximal Ni_p. This Ni is also bridged (via two other cysteines) to a second Ni ion (distal Ni_d); thus, Ni_p is coordinated to three bridging thiolates. Ni_d has an N_2S_2 square-planar environment including coordination to two amide nitrogens derived from the protein backbone.[7−9] Evidence suggests that CO and methyl groups bind to Ni_p during catalysis.[10,11]

Although aspects of the ACS catalytic mechanism remain uncertain, our understanding of it is gradually improving. The components of the A cluster in its most oxidized redox state (called A_{ox}) appear to be in the $\{[Fe_4S_4]^{2+}\ Ni_p^{2+}\ Ni_d^{2+}\}$ electronic configuration.[12,13] This state is inactive for both

(1) Wood, H.G.; Ljungdahl, L.G. *Variations in Autotrophic Life*; Academic Press: London, 1992; pp 201−250.
(2) Grahame, D.A. *Trends Biochem. Sci.* **2003**, *28*, 221−224.
(3) Lindahl, P. A.; Chang, B. *Orig. Life Evol. Biosph.* **2001**, *31*, 403−434.
(4) Lindahl, P. A.; Graham, D. E. In *Nickel and Its Surprising Impact in Nature*"; Sigel, A., Sigel, H., Sigel, R. K. O., Eds.; Metal Ions in Life Science, Vol. 2; John Wiley & Sons, Ltd.: Chichester, UK, 2007; Chapter 9. In press.
(5) Ragsdale, S. W. *Crit. Rev. Biochem. Mol.* **2004**, *39*, 165−195.
(6) Drennan, C. L.; Doukov, T. I.; Ragsdale, S. W. *J. Biol. Inorg. Chem.* **2004**, *9*, 511−515.
(7) Doukov, T. I.; Iverson, T. M.; Seravalli, J.; Ragsdale, S. W.; Drennan, C. L. *Science* **2002**, *298*, 567−572.
(8) Darnault, C.; Volbeda, A.; Kim, E. J.; Legrand, P.; Vernède, X.; Lindahl, P. A.; Fontecilla-Camps, J. C. *Nat. Struct. Biol.* **2003**, *10*, 271−279.
(9) Svetlitchnyi, V.; Dobbek, H.; Meyer-Klaucke, W.; Meins, T.; Thiele, B.; Romer, P.; Huber, R.; Meyer, O. *Proc. Natl. Acad. Sci. U.S.A.* **2004**, *101*, 446−451.
(10) (a) Ragsdale, S. W.; Ljungdahl, L. G.; Dervartanian, D.V. *Biochem. Biophys. Res. Commun.* **1982**, *108*, 658−663. (b) Ragsdale, S. W.; Ljungdahl, L. G.; Dervartanian, D. V. *Biochem. Biophys. Res. Commun.* **1983**, *115*, 658−665. (c) Ragsdale, S. W.; Wood, H. G.; Antholine, W. E. *Proc. Natl. Acad. Sci. U.S.A.* **1985**, 82, 6811−6814.
(11) Barondeau, D. P.; Lindahl, P. A. *J. Am. Chem. Soc.* **1997**, *119*, 3959−3970.
(12) Xia, J. Q.; Hu, Z. G.; Popescu, C. V.; Lindahl, P. A.; Münck, E. *J. Am. Chem. Soc.* **1997**, *119*, 8301−8312.

catalysis and methyl group transfer, but it can be activated by a 2-electron reduction corresponding to an apparent midpoint potential of ca. −540 mV vs NHE at neutral pH.[14] The resulting reductively activated state apparently has the cubane and Ni_d in the 2+ valence, suggesting the unprecedented $\{[Fe_4S_4]^{2+}\text{-}Ni_p^0Ni_d^{2+}\}$ configuration.[12−14] Although the occurrence of a zero-valent Ni atom in the reductively activated state is not established, we will use this nomenclature throughout in this paper, for convenience if for no other reason. For a full discussion of this issue, readers are referred to the literature.[4,13−15] If preferred, "Ni^0" can be viewed simply as an electron-counting formalism indicating the A_{ox} state to which $2e^-$ have been added. This formal view does not complicate or bias any interpretation, analysis, or conclusion presented here.

Whether the methyl group or CO binds first to the enzyme remains contentious, and reasonable arguments have been made for both cases.[5,6,11,16] The one-electron-reduced and CO-bound state of the A cluster (the $S = {}^1/_2$ A_{red}−CO state) has been proposed to be an intermediate of catalysis as well as an inhibitory state. Recent evidence that ACS/CODH need not pass through the A_{red}−CO state during catalysis, and evidence that reductive activation requires 2 electrons[14] compels us to favor the case where the methyl group binds first. It is also known that the reductively activated state accepts a methyl group in the absence of CO, as shown in reaction 2.

$$Ni^0 + CH_3{-}CO^{3+}FeSP \rightleftarrows Ni^{2+}{-}CH_3 + Co^{1+}FeSP \quad K_{met} = \frac{k_{+met}}{k_{-met}} \quad (2)$$

The resulting methylated state is stable and has been characterized.[11,14,17,18] When exposed to CO, e.g. during catalysis, CO is thought to insert into the Ni−methyl bond in accordance with reaction 3.

$$Ni^{2+}{-}CH_3 + CO \rightleftarrows Ni^{2+}{-}C(O)CH_3 \quad K_{ins} = \frac{k_{+ins}}{k_{-ins}} \quad (3)$$

Reaction of the acetyl intermediate with CoA affords acetyl-CoA and regenerates the reductively activated state, reaction 4.

$$Ni^{2+}{-}C(O)CH_3 + CoA \rightleftarrows CH_3C(O){-}CoA + Ni^0 \quad K_{CoA} = \frac{k_{+CoA}}{k_{-CoA}} \quad (4)$$

Reactions 2−4 complete the catalytic cycle for the synthesis of acetyl-CoA.

Of these steps, only methyl group transfer, reaction 2, has been studied specifically.[19−21] In a stopped-flow study, ACS/CODH and Ti^{3+}citrate were preincubated to generate the Ni^0 state, and then reacted against $CH_3{-}Co^{3+}FeSP$ (also preincubated in Ti^{3+}citrate) and monitored at 390 nm where the product $Co^{1+}FeSP$ absorbs. Under these conditions, the reverse of reaction 2 (i.e. starting from $Ni^{2+}{-}CH_3$ and Co^{1+}) could barely be detected, indicating that the equilibrium position lies on the side of the products.[21] In contrast, the reverse reaction proceeded rapidly and to near completion when the $Ni^{2+}{-}CH_3$ was not preincubated with Ti^{3+}citrate. Under these conditions, the equilibrium position appears to be on the side of the reactants of reaction 2. This reductant-dependent shift in the kinetic and thermodynamic properties of the methyl group transfer reaction is not understood mechanistically.

Bhaskar et al. have examined the steady-state kinetics of the exchange reaction between acetyl-CoA and dephospho-CoA as catalyzed by the ACS/CODH homologue from *Methanosarcina barkeri*.[22] Their results indicate a ping−pong mechanism in which the binding of acetyl-CoA to the enzyme is followed by the release of CoA and formation of the acetyl intermediate. They proposed that acetyl-CoA binds to the *oxidized* form of the enzyme, followed by reduction. This was suggested because partially reduced enzyme exhibited cooperative binding with acetyl-CoA, whereas fully reduced enzyme showed simple hyperbolic binding. However, the same behavior would be observed if enzyme were first reduced and then bound with acetyl-CoA. This latter scenario would be congruent with a nucleophilic attack (e.g., by a Ni^0 species) on the carbonyl of acetyl-CoA, as in the reverse of reaction 4. The alternative proposal of binding followed by reduction would seem to require attack by Ni^{2+}, a non-nucleophilic metal ion. Using two methods, Bhaskar et al. measured the equilibrium constant for the reverse of reaction 4 to be ∼0.2 (averaged value),[22] suggesting $K_{CoA} \approx 5$ for a homologous ACS/CODH from a methanogenic archaeon.

To date, no direct studies of the CO insertion, reaction 3, have been reported, nor have the kinetics of the reductive elimination of the acetyl group and CoA, reaction 4, been reported. The problem in studying these reactions has been to identify strategies for monitoring them. Using stopped-flow kinetics, we report here that reactions 3 and 4 can be monitored by starting with the *methylated* state of ACS/CODH. Resulting traces were used to construct a simple kinetic model describing the catalytic mechanism of acetyl-CoA synthase. In this paper we report these results and describe the model.

Experimental Procedures

Preparation of Proteins. *M. thermoacetica* cells were grown and harvested as described previously.[23] ACS/CODH, CoFeSP, and methyl transferase were purified in a glovebox containing <1 ppm O_2.[11,24] Protein concentrations were determined as described previously.[25] Each protein was >90% pure, as quantified by imaging Coomassie blue (Bio-Rad)-stained SDS-PAGE gels (Alpha Innotech Imager 2000). Portions were thawed as needed, subjected to a 1 cm × 20 cm column of Sephadex G25 equilibrated in 50 mM Tris (pH 8.0) + 1 mM dithiothreitol (DTT), divided into aliquots, and either used immediately

(13) Lindahl, P. A. *J. Biol. Inorg. Chem.* **2004**, *9*, 516−524.
(14) Bramlett, M. R.; Stubna, A.; Tan, X.; Surovtsev, I. V.; Münck, E.; Lindahl, P. A. *Biochemistry* **2006**, .
(15) Amara, P.; Volbeda, A.; Fontecilla-Camps, J. C.; Field, M. J. *J. Am. Chem. Soc.* **2005**, *127*, 2776−2784.
(16) Seravalli, J.; Kumar, M.; Ragsdale, S. W. *Biochemistry*, **2002**, *41*, 1807−1819.
(17) Pezacka, E.; Wood, H. G. *J. Biol. Chem.* **1988**, *263*, 16000−16006.
(18) Lu, W.-P.; Harder, S. R.; Ragsdale, S. W. *J. Biol. Chem.* **1990**, *265*, 3124−3133.
(19) Zhao, S.; Roberts, D. L.; Ragsdale, S.W. *Biochemistry* **1995**, *34*, 15075−15083.
(20) Kumar, M.; Qiu, D.; Spiro, T. G.; Ragsdale, S. W. *Science* **1995**, *270*, 628−630.
(21) Tan, X.; Sewell, C.; Lindahl, P. A. *J. Am. Chem. Soc.* **2002**, *124*, 6277−6284.
(22) Bhaskar B.; DeMoll, E.; Grahame, D. A. *Biochemistry* **1998**, *37*, 14491−14499.
(23) Lundie, L. L., Jr.; Drake, H. L. *J. Bacteriol.* **1984**, *159*, 700−703.
(24) Maynard, E. L.; Sewell, C.; Lindahl, P. A. *J. Am. Chem. Soc.* **2001**, *123*, 4697−4703.
(25) Pelley, J. W.; Garner, C. W.; Little, G. H. *Anal. Biochem.* **1978**, *86*, 341−343.

or frozen in liquid N_2. Acetyl-CoA synthase and CO oxidation activities were assayed as described previously.[24] Samples had specific activities of 1.2 μmol min^{-1} mg^{-1} and 400 units mg^{-1}, respectively. EPR of ACS/CODH in the presence of 1 atm CO exhibited the NiFeC signal with a spin intensity corresponding to 0.2 spins/$\alpha\beta$, as determined elsewhere.[26] Ti^{3+}citrate solutions were prepared from $TiCl_3$ (Aldrich) and standardized by titration against $K_3[Fe(CN)_6]$.[27] Co^{1+}FeSP was methylated using CH_3-tetrahydrofolate (THF) (Sigma) and methyltransferase.[11] ACS/CODH was methylated (forming CH_3-ACS/CODH) and then separated using a phenyl sepharose column.[21] In a previous equivalent experiment,[21] CH_3-Co^{3+}FeSP contained 0.95 methyl groups per protein, and ACS/CODH was methylated to the extent of 0.5 CH_3/$\alpha\beta$.

CO Insertion Reaction. A stopped-flow kinetic experiment was performed at 25 °C with an SF-61 DX2 double-mixing instrument and a Xe lamp (Hi-Tech Limited, UK) installed in an Ar-atmosphere glovebox (MBraun) containing <1 ppm O_2. For all experiments in this study, reactions were monitored in PM mode at 390 nm (and, in some cases, at 450 nm). A 3-L Ar-filled flask with a 2-mL conical vial fused at the bottom was sealed with a rubber septum that had been stored in the glove box for >1 wk. An aliquot (1.2 mL) of a 20 μM solution of CH_3-ACS/CODH in Buffer A (50 mM Tris pH 8 + 100 μM DTT) was transferred to a vial. Different volumes of oxygen-scrubbed (Oxysorb cartridge, MG industries) research-grade CO (MG Industries) were injected into the vessel by syringe, affording [CO] of 0, 0.1, 0.5, 1.0, 2.0, and 5.0 μM in each respective flask. The solution was stirred slowly for 4 h, and then transferred to a stopped-flow syringe. The other syringe contained 10 μM of Co^{1+}FeSP and 200 μM of Ti^{3+}citrate in a solution of Buffer A. The experiments were repeated with CO (20 μM) included in the CoFeSP syringe rather than in the ACS/CODH syringe.

Acetyl Group Transfer Reaction. CH_3-ACS/CODH (20 μM in Buffer A) was preincubated for 2 h in the 3-L Ar-filled flask, mentioned above, containing either 20 or 40 μM CO and then was transferred to a stopped-flow syringe. The other syringe contained 10 μM of CH_3-Co^{3+}FeSP and coenzyme A at different concentrations (10, or 100, or 1000 μM, respectively) in a solution of Buffer A.

Acetyl-CoA Synthesis Reaction. A 380-μL solution of Buffer A containing CoA (1.4 mM), CH_3-Co^{3+}FeSP (100 μM), Ti^{3+}citrate (200 μM), CO (100 μM) (all final concentrations) were added to a reaction vessel. The vessel was sealed with a rubber septum, removed from the glovebox, flushed for 15 min with a mixture of Ar and CO (100 μM CO), and returned to the box. To prepare these gases, Ar was passed through an Oxysorb (MG Industries) filter, mixed with equivalently treated CO using a calibrated flow meter (MG Industries, series 7941-AS2 4 tube), and passed into the vessel. The resulting solution was incubated for 15 min at 25 °C in dim light. Acetyl-CoA synthesis was initiated by addition of 20 μL of an ACS/CODH solution (0.2 μM $\alpha\beta$, final). Aliquots (50 μL) were removed by syringe at various times, quenched, and analyzed for acetyl-CoA by reversed phase HPLC.[24] Initial rates were determined by linear least-squares regression analysis of [acetyl-CoA] vs time plots.

Kinetic Model, Simulations, and Fitting. For the model described in the text, a set of ordinary differential equations (ODEs) was generated assuming the *Law of Mass Action*. Once initial concentrations for all species and rate coefficients associated with these reactions were specified, the ODEs were numerically solved using a 4th-order Runge−Kutta method to yield a set of component concentrations at any time. Data were fit using Origin (version 7.5) software. Extinction coefficient changes at 390 nm for reactions 2 and 5 (see below) were given by $\Delta\epsilon_{met} = (\epsilon_{Co1+} + \epsilon_{CH3-Ni} - \epsilon_{CH3-Co} - \epsilon_{Ni0})$ and $\Delta\epsilon_{CO} = (\epsilon_{Ni:CO} - \epsilon_{Ni0})$, respectively, while extinction coefficient changes for reactions 3 and 4 were presumed to be negligible. The values assigned to $\Delta\epsilon_{met}$ and $\Delta\epsilon_{CO}$ were +0.0100 and −0.0015 μM^{-1} cm^{-1}, respectively, which were adjusted slightly from experimentally reported values.[21] Experimental traces of A_{390} were simulated using the expression

$$A_{390}(t) = A_{390}(0) + \Delta\epsilon_{met}\cdot X_{met}(t) + \Delta\epsilon_{CO}\cdot X_{CO}(t)$$

where X_{met} and X_{CO} represent the extent of reactions 2 and 5 at any time.

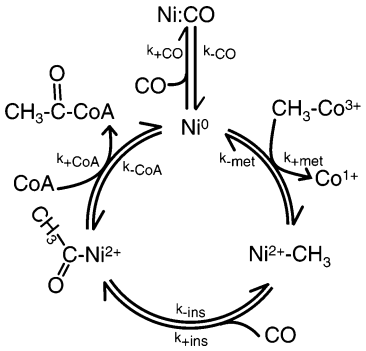

Figure 1. Kinetic model describing the mechanism by which ACS/CODH catalyzes the synthesis of Acetyl-CoA.

Reaction conditions used were common for all experiments (namely 200 μM Ti^{3+}citrate, 50 mM buffer (Tris pH 8), 100 μM DTT occurring at 25 °C), allowing a single consistent set of simulations to be obtained. All rate coefficients and equilibrium constants reported are *apparent* values specifically for these conditions. Concentrations used during the fitting procedure were allowed to differ by ±10% relative to experimentally determined values (except for [CO] which was allowed to vary ±25%). This flexibility corresponds to the relative uncertainty associated with the experimental determinations. ACS/CODH has been reported to be heterogeneous, with active fractions varying between 20 to 50%, depending upon the property measured.[26,28] Since 0.5 methyl groups have been reported to be accepted per ACS/CODH,[11,21] we have assumed this value for all simulations. The [ACS/CODH] given for the experiments described in the text refer to experimentally determined concentrations of the $\alpha\beta$ dimer, assuming a molecular mass of 154 kDa, whereas [ACS/CODH] concentrations assumed for simulations were *half* of the experimental values.

Results

While analyzing the experiments described below, we developed a simple but comprehensive kinetic model that describes how ACS/CODH catalyzes the synthesis of acetyl-CoA from CO, CoA, and CH_3-Co^{3+}FeSP. This model, illustrated in Figure 1, consists of reactions 2, 3, 4 and an inhibition step, reaction 5.

$$Ni^0 + CO \rightleftarrows Ni{:}CO \qquad K_{CO} = \frac{k_{+CO}}{k_{-CO}} \tag{5}$$

The nomenclature Ni:CO leaves ambiguous the oxidation state of the proximal Ni in the inhibited form and the issue of whether CO is bound directly to the Ni in that form.

Methyl Group Transfer Reaction. Although the kinetics of methyl group transfer have been evaluated previously,[21] we re-evaluated this reaction for the particular batch of enzyme used. A solution of ACS/CODH and Ti^{3+}citrate was placed in one syringe and a solution of CH_3-Co^{3+}FeSP and Ti^{3+}citrate was place in the other. Upon mixing, changes in the absorbance at 390 nm were monitored vs time, and an analytical expression

(26) Shin, W. S.; Anderson, M. E.; Lindahl, P. A. *J. Am. Chem. Soc.* **1993**, *115*, 5522−5526.
(27) Seefeldt, L. C.; Ensign, S. A. *Anal. Biochem.* **1994**, *221*, 379−386.
(28) Fraser, D. M.; Lindahl, P. A. *Biochemistry* **1999**, *38*, 15697−15705.

for bimolecular reaction 2 was used to fit the resulting experimental traces (data not shown). The best-fit forward rate coefficient (k_{+met} =15 μM^{-1} s^{-1}) was within error of that reported previously, while the reverse rate coefficient (k_{-met} = 0.05 μM^{-1} s^{-1}) was ~30 times less than the previous estimate.[21] The ratio of these two rate coefficients affords the equilibrium constant $K_{met} \approx 300$. Similar to the previous study, the reverse reaction proceeded rapidly and extensively as long as the $Ni^{2+}-CH_3$ state was not preincubated with Ti^{3+}citrate. In this case, the kinetic parameters were $k_{+met} = 0.13$ μM^{-1} s^{-1} and $k_{-met} = 1.8$ μM^{-1} s^{-1} affording $K_{met} \approx 0.07$.[29]

CO Insertion Reaction. Our next objective was to determine the equilibrium constant for reaction 3, in which CO inserts into CH_3-ACS/CODH. A solution of CH_3-ACS/CODH was *preincubated* with CO in one syringe and then reacted with a solution of Co^{1+}FeSP while monitoring the absorbance at 390 nm. Depending on the [CO] and the magnitude of K_{ins}, the syringe that initially contained CO and CH_3-ACS/CODH should, by the time it is mixed with Co^{1+}FeSP, contain equilibrium proportions of CH_3-ACS/CODH and $CH_3C(O)-$ACS/CODH. Since only the CH_3-ACS/CODH form can donate a methyl group to Co^{1+}FeSP, the initial rate of reaction will reflect the proportion of ACS/CODH in this form. In the absence of CO, all of the enzyme will be in the CH_3-ACS/CODH form, and the rate of reverse methyl transfer (and requisite decline at 390 nm) will be maximal. At infinite [CO], all of the enzyme will be in the $CH_3C(O)-$ACS/CODH form, and no methyl transfer will be observed.

Preliminary experiments revealed that even at concentrations of CO comparable to those of ACS/CODH used, the CO insertion reaction product was almost quantitatively formed. Thus, the experiment was repeated in a large vessel such that the final concentration of free CO was virtually identical to the added concentration of CO, regardless of the amount of CO that associated with the enzyme. The results (Figure 2A) displayed the expected behavior. In Panel B, initial rates v_0 of this reaction are plotted vs [CO]. These data-points were determined from the expression $v_0 = \Delta A_{390}/(\Delta t \cdot \Delta \epsilon_{met})$ where ΔA_{390} is the initial absorbance change and Δt is the initial time interval. For the rates shown in Figure 2B, Δt corresponds to the first 0.05 s of reaction. The solid line in Figure 2B is the best-fit of expression 6 to the data,

$$v_0 = k_{-met}[CO^{1+}FeSP]_0[Ni^{2+}-CH_3]_0 \frac{K_{D(ins)}}{[CO] + K_{D(ins)}} \quad (6)$$

affording the dissociation constant for the CO insertion reaction 3, $K_{D(ins)} = 1/K_{ins} = 0.31 \pm 0.11$ μM. $[Co^{1+}FeSP]_0$ and $[Ni^{2+}-CH_3]_0$ refer to the active concentrations of these proteins initially present after mixing, while [CO] is concentration of CO in the pre-equilibration solution. Derivation of eq 6 does not include reactions 4 and 5 since no CoA was present in the experiment and the concentration of CO used was very low. It assumes that reaction 3 had reached equilibrium prior to reaction with Co^{1+}FeSP.

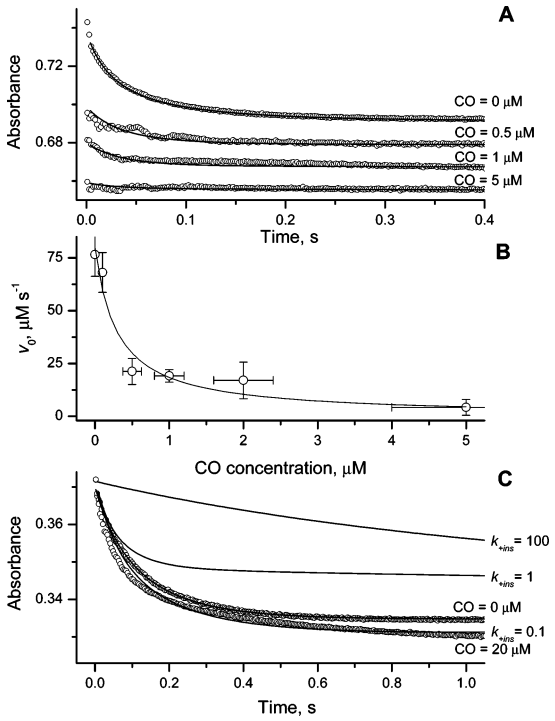

Figure 2. Stopped-flow reaction of CH_3-ACS/CODH with CO and Ti^{3+}-citrate-reduced Co^{1+}FeSP. (A) CO was pre-equilibrated in the CH_3-ACS/CODH syringe. (○) Experimental traces of A_{390} vs time using indicated [CO]. (—) Simulations using the model of Figure 1 and the kinetic parameters given in Table 1 except $k_{+met} = 0.13$ μM^{-1} s^{-1} and $k_{-met} = 1.8$ μM^{-1} s^{-1}. (B) (○) Initial rates obtained as described in the text. (—) Best-fit of eq 6, obtained using $K_{D(CO)} = 0.31$ μM. Error bars reflect the estimated uncertainties for each point. (C) CO initially in the Co^{1+}FeSP syringe. (○) Experimental traces of A_{390} vs time. (—) Simulations with kinetic parameters as in A, except k_{+ins} values of 100, 1, and 0.1 μM^{-1} s^{-1}.

Our next objective was to explore the kinetics of reaction 3. To do this, CH_3-ACS/CODH was included in one stopped-flow syringe, while Co^{1+}FeSP and CO were included in the other. If CO inserted at an infinitely fast rate relative to that of the reverse methyl transfer reaction (reaction 2, right to left), the resulting acetyl form would not react with Co^{1+}FeSP, and no absorbance decline at 390 nm would be observed. On the other extreme, if CO inserted at an infinitely slow rate, CH_3-ACS/CODH would react with Co^{1+}FeSP, and A_{390} would decline rapidly. As shown in Figure 2C, A_{390} declined at a rate similar to that observed in the absence of CO. These traces were simulated assuming the model of Figure 1, the set of experimentally determined concentrations, and the $k_{+met(no\ red)}$, $k_{-met(no\ red)}$ and $K_{D(ins)}$ values determined above, as well as the other parameters determined below and listed in Table 1. Numerous simulations were generated using various trial values for all other required parameters. The resulting simulations (solid lines nearest to the experimental traces) were obtained using the set of kinetic parameters described below. The other solid lines in Figure 2C were generated using the same parameters except for the indicated values of k_{+ins}. The lack of fidelity to the data indicates that the rate of CO insertion is relatively slow under the conditions of this experiment.

(29) We previously estimated a value of 2.3 for the equilibrium constant associated with methyl group transfer.[21] Although we mentioned in that report that forward and reverse rate constants depended on the presence/absence of reductant, we calculated the equilibrium constant using the *forward* rate constant as determined in the *presence* of reductant and the *reverse* rate constant as determined in the *absence* of the reductant. In hindsight, a more reasonable approach, which we take here, would have been to report two K_{met} values, one relevant for reactions performed in the presence of a reductant, one for reactions performed in the absence of a reductant. Our calculated respective values, $K_{met} \approx 300$ and $K_{met(no\ red)} \approx 0.07$, indicate that, in the presence of reductant, the methyl group transfer reaction at equilibrium lies far to the side of the products, whereas in the absence of a reductant it lies far to the side of the reactants. The kinetic model developed here reflects the situation in the presence of reductant, as is typical of ACS/CODH catalytic reaction conditions.

Table 1. Kinetic Parameters used in Fitting

$k_{+met} = 15.0 \pm 1.8\ \mu M^{-1}\,s^{-1}$	
$k_{-met} \leq 0.05\ \mu M^{-1}\,s^{-1}$	$K_{+met} \geq 300$
$k_{+ins} = 0.11 \pm 0.08\ \mu M^{-1}\,s^{-1}$	
$k_{-ins} = 0.033\ s^{-1}$	$K_{-ins} = 3.3 \pm 1.1\ \mu M^{-1}$
$k_{+CoA} = 3.8 \pm 1.0\ \mu M^{-1}\,s^{-1}$	
$k_{-CoA} = 5.8 \pm 2.7\ \mu M^{-1}\,s^{-1}$	$K_{CoA} = 0.66$
$k_{+CO} = 12.5 \pm 7.8\ \mu M^{-1}\,s^{-1}$	
$k_{-CO} = 64.8 \pm 9.4\ s^{-1}$	$K_{CO} = 0.19\ \mu M^{-1}$

Acetyl Group Transfer Reaction. To monitor reaction 4, a solution containing $Ni^{2+}-CH_3$ and CO was placed in one stopped-flow syringe, while a solution of CH_3-Co^{3+}FeSP and CoA was placed in the other. The concentration of CO in the syringe was in all cases sufficient for ~99% of ACS/CODH to be acetylated given $K_{D(ins)} = 0.31\ \mu M$. The concentration of CoA was varied from 10 to 1000 μM. Reactions were monitored at 390 nm (Figure 3) and at 450 nm (data not shown); equivalent results were obtained. At low [CoA] (Figure 3C), the reaction of CoA with the acetyl intermediate was relatively slow such that a small amount of Ni^0 was generated soon after mixing. Consequently, the rate by which Ni^0 methylated (as monitored by the increase at A_{390}) was slow. At the highest [CoA] used, the reaction of CoA with the acetyl intermediate was sufficiently fast such that a larger proportion of the enzyme was converted into the Ni^0 state, and this large proportion could be methylated, resulting in a more rapid rise of A_{390} (Figure 3A). The rate at which A_{390} increased for the experiment with an intermediate [CoA] (Figure 3B) was intermediate of that observed in traces A and C.

The experimental traces exhibited two distinctive features. First, the extent of reaction was similar in all three experiments, suggesting that the equilibrium position of the ACS reaction lies on the product side. Second, the rate of the apparent reaction for methyl group transfer depends *weakly* on [CoA], in that the order-of-magnitude changes in [CoA] only altered the rates of reaction by factors of ~2.

Data collected for the acetyl group transfer reaction were initially analyzed using a minimal kinetic scheme consisting solely of reactions 2 and 4. Reaction 3 was neglected because it should have reached equilibrium before the content of the two syringes were mixed. This scheme failed to reproduce all experimental traces simultaneously using a common set of kinetic parameters (it allowed each trace to be fitted separately and with a unique set of parameters). Even with reaction 3 included, fits were unacceptable. The model was modified by assuming that CoA inhibited the reaction by binding to the Ni^0 form, but fits were unimproved (data not shown). Reaction 4 was decomposed into two to three separate steps (reflecting separate binding, reaction, and/or dissociation steps); this improved fits marginally but not to our satisfaction. Finally, we augmented reactions 2−4 with a reaction in which CO binds to the Ni^0 form, reaction 5. This model fit well to the data, yielding the simulations shown as the solid lines in Figure 3A−C, obtained using the kinetic parameters given in Table 1. Note that the values for k_{+met} and k_{-met} are those obtained for the methyl group transfer reaction under reducing conditions.

The model and kinetic parameters obtained above predicted significant inhibition of acetyl-CoA synthesis by CO binding to enzyme. The inhibitory effect of CO was confirmed in trace D of Figure 3, where [CO] = 40 μM (and [CoA] = 1000 μM).

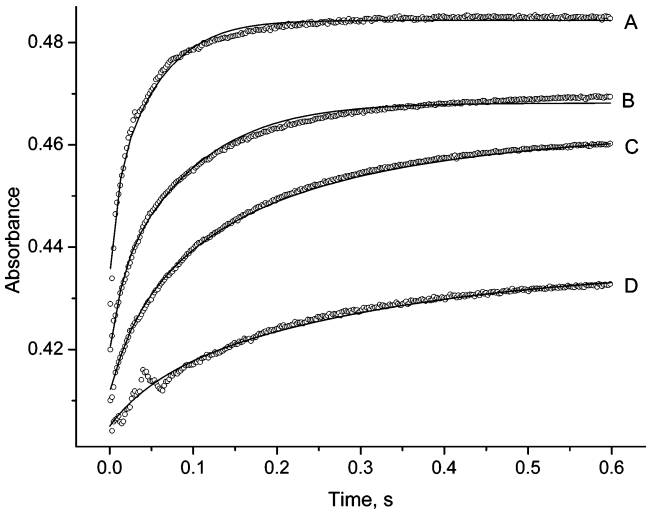

Figure 3. Stopped-flow reaction of the acetylated ACS/CODH intermediate with CoA and subsequent reaction of the reductively activated state with CH_3-Co^{3+}FeSP. (○), experimental data. In A, B, and C, the [CO] was 20 μM and the [CoA] was 1000, 100, and 10 μM, respectively. In (D) [CO] was 40 μM, and [CoA] was 1000 μM. (—) Simulations using the model of Figure 1 with kinetic parameters listed in Table 1.

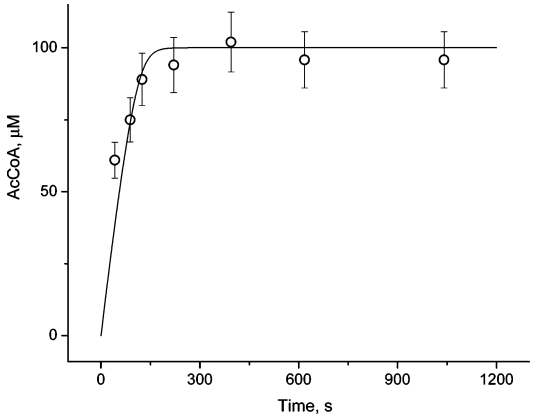

Figure 4. Acetyl-CoA synthesis. (○), Acetyl-CoA; (—) Simulation using the model of Figure 1, kinetic parameters listed in Table 1, and experimental concentrations. Error bars reflect the estimated uncertainties for each point.

The solid line of Figure 3D is a simulation using the concentrations for the experiment and the kinetic parameters listed in Table 1.

Acetyl-CoA Synthesis. The equilibrium constant for the synthesis of acetyl-CoA, K_{ACS} of reaction 1, equals the product of the equilibrium constants for three constituent reactions as given by the relationship $K_{ACS} = K_{met} \cdot K_{ins} \cdot K_{CoA}$. Our simulations afforded values for the three equilibrium constants contributing to this relationship (listed in Table 1), suggesting that K_{ACS} is greater than ~660 μM^{-1} (300·3.3 μM^{-1}·0.66). We estimated K_{ACS} experimentally as a means of testing our model and these values. The concentration of acetyl-CoA produced at different times during an acetyl-CoA synthase assay was determined by HPLC as the reaction was allowed to continue to equilibrium. As shown in Figure 4, the final amount generated (98.5 μM ± 1.5 μM, starting with 100 μM of CH_3-Co^{3+}FeSP) indicates that the reaction proceeds to completion within the uncertainty of the measurement. The curve was simulated using a model composed of the bimolecular reaction obtained from reaction 1 after assuming a fixed [CO] = 100 μM (as was the case during the experiment). Best-fit kinetic parameters were $k_+ = 0.00086$

μM^{-1} s^{-1} and $k_- = 0.00039$ μM^{-1} s^{-1}, indicating that $K_{ACS} = 0.00086/0.00039/100 = 0.02$ μM^{-1}. A value of $K_{ACS} = 0.05$ μM^{-1} was obtained using experimental equilibrium concentrations. Given the uncertainty of these measurements, combined with the fact that the equilibrium position is far to the side of the products, we can conclude only that the *lower limit* of K_{ACS} is ~ 0.02 μM^{-1}. Thus, these estimates are entirely consistent with the value of K_{ACS} calculated from the kinetic parameters reported here.

Discussion

This is the first study to report on the kinetics of the CO insertion and acetyl group transfer steps occurring within the ACS catalytic mechanism. This achievement was obtained using the stopped-flow kinetic method and by beginning with the methylated intermediate form of the enzyme. Reactions were monitored indirectly, using the methyl group transfer reaction to/from the CoFeSP as a "reporter" reaction monitorable at both 390 and 450 nm (we chose to monitor at 390 nm for reasons of increased sensitivity). In these reactions, ACS/CODH and CoFeSP were always placed in different stopped-flow syringes, while CO and CoA were strategically placed in either syringe such that the reaction of interest would occur in a manner that could be reported at 390 nm.

The complexity of these arrangements required that the resulting traces be simulated computationally. In turn, this led to the construction of a comprehensive kinetic model of catalysis using chemical rate coefficients. Constructing such models is uncommon in contrast to the steady-state analysis of an enzyme mechanism using combinations of such kinetic parameters. The rarity of microscopic kinetic models is due to the difficulty (often the impossibility) of monitoring each step of a mechanism and of globally fitting the kinetic traces obtained. If the number of unknown parameters is excessive relative to the experimental data available, such systems will be underdetermined and lack predictive value. We have minimized this problem by obtaining data sensitive to each step of catalysis and by restricting the complexity of the model. Thus, we have not explicitly included a step in which the α subunit undergoes an open:closed conformational change[30] nor have we taken into account the presence of the residual catalytic activity which probably reflects the direct binding of CO in solution to Ni_p.[24,31−32] The kinetic model developed here reflects the majority activity in which CO serves as both substrate and inhibitor.

As illustrated in Figure 1, our model consists of four reactions, including reactions 2−5, the first three of which combine to afford the overall ACS reaction 1. The parameters obtained by fitting to the experimental traces reported here indicate that the equilibrium position of the methylation reaction 2 lies far to the side of the products. This is consistent with the superior nucleophilic tendency of Ni^0 (or whatever species on which ACS/CODH is attacking) relative to the Co^{1+} cobalamin. Given the complexity inherent in the redox-dependent changes in kinetic and thermodynamic parameters for the methyl group transfer reaction, our model is restricted to catalytic processes

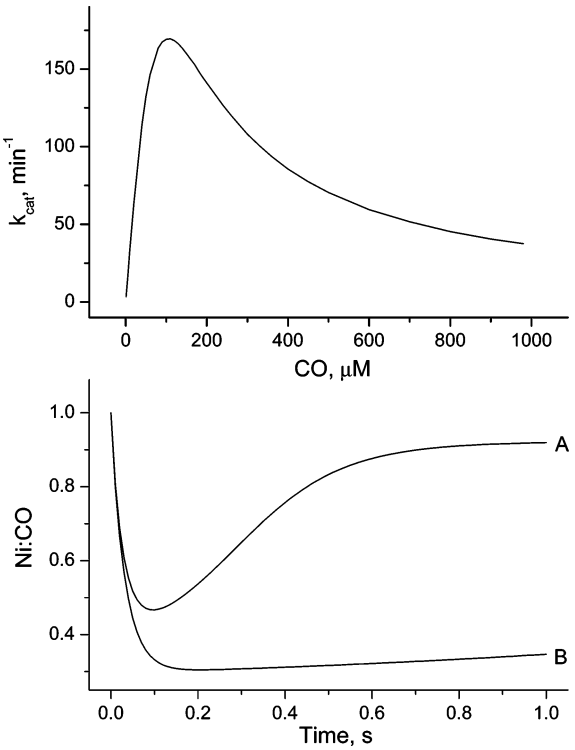

Figure 5. Simulation of acetyl-CoA activity under different reaction conditions. (Upper Panel) [ACS/CODH] = 0.5 μM (active); [CH_3−Co^{3+}-FeSP] = 30 μM; [CoA] = 1000 μM. Simulations were obtained assuming these concentrations, the model of Figure 1 and the kinetic parameters of Table 1, except for $K_{D(CO)}$ which was set to 2.8 μM. Velocities were determined at 0.3 s reaction time. (Lower Panel) Simulated plot of the fraction of ACS/CODH in the Ni:CO form vs time, using the parameters of Table 1 without exceptions. (A) [ACS/CODH] = 25 μM (active); [CH_3−Co^{3+}FeSP] = 30 μM; [CoA] = 500 μM; [CO] = 120 μM. (B) Same as A except [ACS/CODH] = 2.5 μM (active).

under reducing conditions. CO is involved in two reactions, namely as a substrate in the CO insertion step 3 and as an inhibitor in the CO binding step 5. According to these values, when CO inserts, it binds over 10-fold more tightly than when it inhibits. The equilibrium position of the acetyl-transfer reaction 4 lies slightly to the side of the reactants, in contrast to the ACS/CODH homologue from *M. barkeri*, for which the equilibrium constant is 7 times greater.[22]

A major advantage of a comprehensive kinetic model of an enzyme-catalyzed reaction is that it can be used to quantitatively predict the behavior of the enzyme under any set of substrate, product, and enzyme concentrations. There are two well-known properties of ACS/CODH catalysis against which we wanted to test the model developed here. The variation of ACS activity with substrate [CO] is not simply the hyperbolic curve predicted by the Michaelis−Menten equation; in the case of ACS/CODH, initial velocity divided by total ACS/CODH concentration increases to ~ 100 min^{-1} as [CO] increases from 0 to ~ 100 μM, but then it *declines* as [CO] increases to 980 μM (1 atm).[24] A set of simulations was obtained at different [CO] using our model. The concentrations of species used for the simulations were those used experimentally to generate the curve just described. The kinetic parameters used were those given in Table 1 except for $K_{D(CO)}$ which was set to 2.8 μM rather than 5.2 μM. The plot of the simulated initial rate of product formation (v_0/[ACS/CODH]$_{tot}$) vs [CO] revealed behavior reminiscent of that observed experimentally (Figure 5A, upper panel). This

(30) Tan, X.; Bramlett, M. R.; Lindahl, P. A. *J. Am. Chem. Soc.* **2004**, *126*, 5954−5955.
(31) Tan, X.; Loke, H.-K.; Fitch, S.; Lindahl, P. A. *J. Am. Chem. Soc.* **2005**, *127*, 5833−5839.
(32) Tan, X.; Volbeda, A.; Fontecilla-Camps, J. C.; Lindahl, P. A. *J. Biol. Inorg. Chem.* **2006**, *11*, 371−378.

includes a maximal rate near ~100 min^{-1} occurring at [CO] ≈ 100 μM. The exact magnitude and position at which maximal activity occurred could be adjusted by changing the value of $K_{D(CO)}$. The steepness in the decline of activity with increasing [CO] beyond the optimal [CO] was less than that observed experimentally, perhaps because CO inhibition may be cooperative,[24] an effect not currently included in our simple model.

A second well-established behavior of ACS/CODH catalysis is that the A_{red}−CO state (which exhibits the NiFeC EPR signal[10]) decays when enzyme prepared in this state (by incubation in CO) is reacted with CH_3-Co^{3+}FeSP.[11,16,33] Under the conditions of their experiment, with CoA included to complete the catalytic cycle, Seravalli et al. reported that the signal decays within ~1 s followed by a plateau region in which ~33% of the spectral intensity remains over the course of 10 s.[16] They took this plateau as evidence that the A_{red}−CO state is a catalytic intermediate. The plateau was viewed as resulting from a steady-state condition where the rate at which the A_{red}−CO state formed from the previous catalytic intermediate matched that at which the A_{red}−CO state converted into the subsequent intermediate. However, simulations obtained using our model, where the *inhibitory* Ni:CO state was presumed to reflect the A_{red}−CO state, also reproduced the essential features of this behavior (Figure 5, lower panel). The duration and flatness of the plateau region in our simulations could be adjusted by changing the concentrations of ACS/CODH and CoFeSP. Simulation A was obtained using the reported experimental conditions, whereas simulation B was obtained by adjusting the [ACS/CODH] to achieve a plateau region more characteristic of that reported. According to our model, this region is never truly flat in CO atmospheres, as it inevitably curves upward as the reaction reaches equilibrium and as the A_{red}−CO state increases in proportion.

The form of the enzyme labeled "Ni:CO" in our model has not been physically characterized, and thus it may or may not correspond to the A_{red}−CO state. Neither the site at which CO binds nor the oxidation state of the Ni in the Ni:CO form are established. All that is known about this kinetic state is that it is generated by adding CO to ACS/COOH in the state present *after* acetyl-CoA is released and *before* a methyl group binds and that it is an inhibitory state of catalysis (i.e., it does not lead to products) that competes with the substrate CH_3-Co^{3+}FeSP for the same state of the enzyme. Within those constraints, there are of course many possibilities. However, it is significant that the Ni:CO state and the A_{red}−CO state have similar dissociation constants ($K_{D(CO)} \approx 5$ μM for the Ni:CO state and 3 μM for the A_{red}−CO state[34]), as would be expected if the two states were identical.

If the Ni:CO and A_{red}−CO states were identical, the ability of our kinetic model to recapitulate the major aspects of ACS/CODH catalytic behavior would represent yet another argument against mechanisms in which the A_{red}−CO state is an intermediate of catalysis. During the review of this manuscript, a reviewer's comment prompted us to consider the mechanistic implications of the fact that ACS/CODH, *in the absence of any other protein*, catalyzes the exchange of the carbonyl group of acetyl-CoA with free CO,[35] reaction 7.

$$CH_3{}^*C(O)\text{-CoA} + CO \rightleftarrows CH_3C(O)\text{-CoA} + {}^*CO \qquad (7)$$

According to the mechanism proposed here, acetyl-CoA would react with Ni^0 (in the manner of reaction 4) to form the acetylated intermediate, $Ni^{2+}-{}^*C(O)CH_3$, which would decarbonylate (reaction 3) to yield $Ni^{2+}-CH_3$ and *CO. Radiolabeled *CO would then exchange with unlabeled CO and reform the unlabeled product by proceeding in the reverse direction. In contrast, mechanisms in which CO bound to the enzyme before the methyl group bound would require that *CO dissociate after the methyl group was transferred from $Ni^{2+}-{}^*C(O)CH_3$. However, in the absence of CoFeSP, the methyl group could not transfer, and thus, no exchange could occur. This argument would become less unambiguous if a small amount of contaminating CoFeSP were included in ACS/CODH preparations (indeed, we often have a trace of the CoFeSP present in our preparations). However, in the seminal paper where this exchange reaction was discovered, Ragsdale and Wood argued forcefully[35] that the only protein contained in their exchange-active preparations was ACS/CODH. Thus, we regard the argument presented here as definitive in disqualifying mechanisms in which CO bind ACS/CODH before the methyl group binds.

Table 2. Sensitivity of the Overall Initial Velocity to Relative Changes in Individual Rate Coefficients

rate coefficient	$(\Delta v_0/v_0)/(\Delta k/k)$
k_{+met}	0.339
k_{-met}	−0.002
k_{+ins}	0.657
k_{-ins}	−0.0004
k_{+CoA}	0.002
k_{-CoA}	0.001
k_{+CO}	−0.332
k_{-CO}	0.317

Another advantage to developing a microscopic kinetic model of an enzymatic process is the ability to identify the degree to which each step in that process controls the overall rate of reaction. To evaluate this issue, we fixed the reactant and enzyme concentration at the values commonly used to assay the enzyme (i.e., [CO] = 100 μM; [CH_3Co^{3+}FeSP] = 30 μM; [CoA] = 1000 μM, [ACS/CODH] = 0.5 μM (active fraction)) and then calculated the percentage of the enzyme in each intermediate state. Our results (Ni^0, 0.2%; $Ni^{2+}-CH_3$, 95%; $Ni^{2+}-C(O)CH_3$, 0.3%; and Ni:CO, 4.4%) indicate that the overwhelming proportion of the enzyme is in the methylated intermediate state. Next, we calculated the relative change in reaction velocity with respect to a relative change in the rate coefficient associated with each step. Our results, given in Table 2, indicate that changes in the rate coefficient associated with the CO insertion step leads to the greatest relative change in reaction velocity. Other reactions with a significant impact on the overall rate include the forward methyl transfer rate and both forward and reverse rates of CO binding. Since intermediates tend to accumulate just prior to the rate-determining step of a multistep process, the accumulation of $Ni^{2+}-CH_3$ and the sensitivity of k_{+met} in affecting the rate both suggest that *the rate-determining step of ACS catalysis is CO insertion*. This step may in reality include a number of distinguishable substeps, only one of which needs to be slow. The only requirement is that these steps occur *after* the methylated intermediate forms

(33) Grahame, D. A.; Khangulov, S.; DeMoll, E. *Biochemistry* **1996**, *35*, 593−600.
(34) Russell, W. K.; Lindahl, P. A. *Biochemistry* **1998**, *37*, 10016−10026.
(35) Ragsdale, S. W.; Wood, H. G. *J. Biol. Chem.* **1985**, *260*, 3970−3977.

and *before* the acetylated intermediate develops. Substeps might include: (a) the dissociation of the Co^{1+}FeSP from CH_3-ACS/CODH; (b) a conformational change in the α subunit which might allow CO to migrate toward Ni_p through a tunnel; (c) the binding of CO to the $Ni^{2+}-CH_3$ species just prior to insertion; and (d) the insertion reaction itself. Efforts are underway to formulate experiments that could provide evidence for these substeps and identify which of them is slow, but we would not be surprised if the slow substep corresponded to either the dissociation of CoFeSP or the conformational change of the α subunit (or to a concerted step involving both processes).

Acknowledgment. This work was supported by the National Institutes of Health (GM46441) and the Robert A. Welch Foundation (A-1170).

JA0627702